Exercises in PET Image Reconstruction

Oliver Nix

Abstract These exercises are complementary to the theoretical lectures about positron emission tomography (PET) image reconstruction. They aim at providing some hands on experience in PET image reconstruction and focus on demonstrating the different data preprocessing steps and reconstruction algorithms needed to obtain high quality PET images. Normalisation, geometric-, attenuation- and scatter correction are introduced. To explain the necessity of those some basics about PET scanner hardware, data acquisition and organisation are reviewed. During the course the students use a software application based on the STIR (software for tomographic image reconstruction) library [1,2] which allows them to dynamically select or deselect corrections and reconstruction methods as well as to modify their most important parameters. Following the guided tutorial, the students get an impression on the effect the individual data precorrections have on image quality and what happens if they are forgotten. Several data sets in sinogram format are provided, such as line source data, Jaszczak phantom data sets with high and low statistics and NEMA whole body phantom data. The two most frequently used reconstruction algorithms in PET image reconstruction, filtered back projection (FBP) and the iterative OSEM (ordered subset expectation maximation) approach are used to reconstruct images. The exercise should help the students gaining an understanding what the reasons for inferior image quality and artefacts are and how to improve quality by a clever choice of reconstruction parameters.

Keywords: PET · sinogram · corrections · tomographic reconstruction · FBP · OSEM

O. Nix
Deutsches Krebsforschungszentrum Heidelberg, Dep. for Medical Physics in Radiology, Im NeuenheimerFeld 28069120 Heidelberg, Germany
e-mail: O.Nix@dkfz-heidelberg.de

Y. Lemoigne, A. Caner (eds.) *Molecular Imaging: Computer Reconstruction and Practice*, 131

1 Introduction

1.1 PET-Scanner Hardware

In PET (Positron Emission Tomography) two back to back emitted photons with an energy of 511 keV emerging from the annihilation of a positron originating from a β^+ decaying nucleus with an electron are detected. In most commercially available PET scanners they are detected using a scintillating material like BGO (bismuth germanate) or more recently GSO (gadolinium oxyorthosilicate) and LSO (lutetium oxyorthosilicate). Usually the block shaped scintillator material is segmented into a matrix of individual elements. The photon deposits energy, mainly by scattering, in the scintillator which is converted to scintillation light that is read out and converted to an electric signal using PMTs (photomultiplier tubes). More recently compact APDs (avalanche photo diode) are used, especially in dedicated PET scanner for small animal imaging. In a typical clinical PET scanner such as the Siemens/CTI EXACT HR+[3] the BGO scintillator material is segmented into arrays of 8×8 read out by four photomultiplier tubes. Due to light sharing between the individual photomultipliers the position of the impacting photon can be estimated using a center of gravity algorithm. The combination of scintillator and photomultiplier is called block detector. They are arranged as one or many rings around the subject. In case of the EXACT HR+ scanner four rings of block detectors exist, each equipped with 72 blocks. In total, this results in 576 channels for each of the 32 rings. In the early days of PET a lead shield, the septa, was positioned between detector rings to prevent the detection of coincident photons between different rings. With the septa inside the FoV (field of view) the data is reduced to a set of 2D planes. This constraint can be dropped for modern PET scanners due to increased computing power and storage capabilities together with the solution to the problem of integrating oblique slices in respect to the z-axis into the tomographic reconstruction process. Data acquisition in so called 3D mode became possible. The data used during the exercises were acquired in 3D mode which is today's standard.

1.2 Data Organisation in PET

The quantities measured in PET are photon energy, position and time. A line of response (LoR) is constructed if both photons have been detected in two different detectors within a certain time and energy window. The LoR can be considered a straight line between the two detectors located somewhere on the PET detector ring. The information content is that a PET event occurred somewhere along this line. Two approaches exist to store this data – listmode and matrix representation. In listmode format all detected events are written to an event list. In addition to the mentioned data additional information like gantry state or if available depth of interaction information can be stored. The listmode data format conserves all

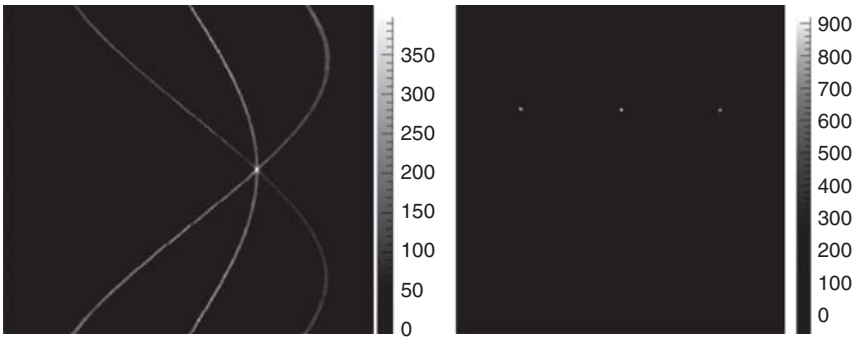

Fig. 1 Left hand side shows the sinogram resulting from three lines sources. Right hand side shows the image reconstructed from this sinogram

information available. It can be integrated in the reconstruction process to increase image quality. In matrix representation only a binary information about the event is kept, that is, that an event fulfilling the imposed criteria occurred in a given LoR. List mode format is mainly used in a research context and for experimental scanner systems while matrix representation is used in clinical routine. Any LoR within one plane can be defined by two coordinates – the tangent distance (x_r) from the center of a plane and an angle (ϕ). Matrix based image reconstruction nearly always starts from projections. A projection is defined by assembling all LoRs within one plane with a fixed angle ϕ. For a set of planes perpendicular to the z-axis the z-coordinate (z) is needed as additional coordinate to define the LoRs. This is the 2D PET case. In 3D PET planes with an arbitrary angle toward the z-axis are allowed. Therefore, a fourth coordinate is introduced to describe the LoRs. The obliqueness (δ) in respect to the z-axis. Planes with similar obliqueness are merged to reduce the data volume. This is effectively equivalent to an axial compression and the merged sinograms are sometimes called segments. Projections can be even if the center of the tomograph is located between two projection bins or odd otherwise. Frequently interleaving between two neighbouring projections is applied. That is merging one neighbouring odd and even projection thus halving the tangential sampling distance. Projections are assembled to sinograms by grouping the projections associated with one z-coordinate such that each row represents one projection. An example of the sinogram resulting from imaging a set of three line sources is shown in Fig. 1. The sinogram is the most widely used representation of PET data.

1.3 Data Acquired During a PET Scan

During a clinical PET scan a progression of emission and transmission scans is performed. During the emission scan the coincident photon events from the β^+ decaying radiotracer and the subsequent e^+e^- annihilation are recorded and stored in

sinogram format. The activity distribution, that is the image, is reconstructed from this data. During the transmission scan a set of rod sources, usually ^{68}Ge, rotate around the subject. The transmission scan is similar to a CT scan except for using 511 keV photons and in comparison very low statistics. The transmission data is used to reconstruct an attenuation image or μ-map. No or only very little anatomical details can be seen on these images. Its sole purpose is to correct for photon attenuation inside the patient's body. Transmission data is again stored as sinograms. In combination with a blank scan which is a transmission scan acquired without any object inside the field of view, the attenuation image can be reconstructed. The blank scan is usually acquired over night as part of daily quality assurance procedures.

2 Corrections on PET Data

It is necessary to preprocess the data before running the actual reconstruction algorithm. A lack of these corrections results in deterioration of image quality and causes typical artefacts depending on the type of correction.

2.1 Normalisation

Normalisation is needed to correct for different efficiencies individual LoRs have. The total efficiency of a LoR is the product of detection efficiency, dead time efficiency and geometrical efficiency. In case of the EXACT HR+ scanner the efficiencies are represented as matrices of floating point numbers stored in a binary normalisation file. They are calculated from high statistic scans of a homogenous cylinder phantom or a line source during normalisation procedures performed approximately every two months. A copy of the normalisation data is added to the patient data record. The normalisation file provided for the exercises contain 32 * 576 scintillator efficiency factors and 63 * 288 geometrical efficiency factors. In addition crystal interference corrections need to be applied to take care for effects originating from the use of block detectors to construct the PET detector ring. A lack of normalisation can be detected easily by looking at the sinograms. In case of non normalised data the sinograms look coarse and channels with significant higher or lower efficiencies can be identified as lines with significantly different amplitudes or in graphical representation grey values. Normalised sinograms appear smoother. Figure 2 shows a non normalised sinogram acquired during a scan of the NEMA whole body phantom and the same data with normalisation applied. The image reconstructed from the non normalised sinogram shows strong ring like artefacts. These structures disappear if normalisation is applied.

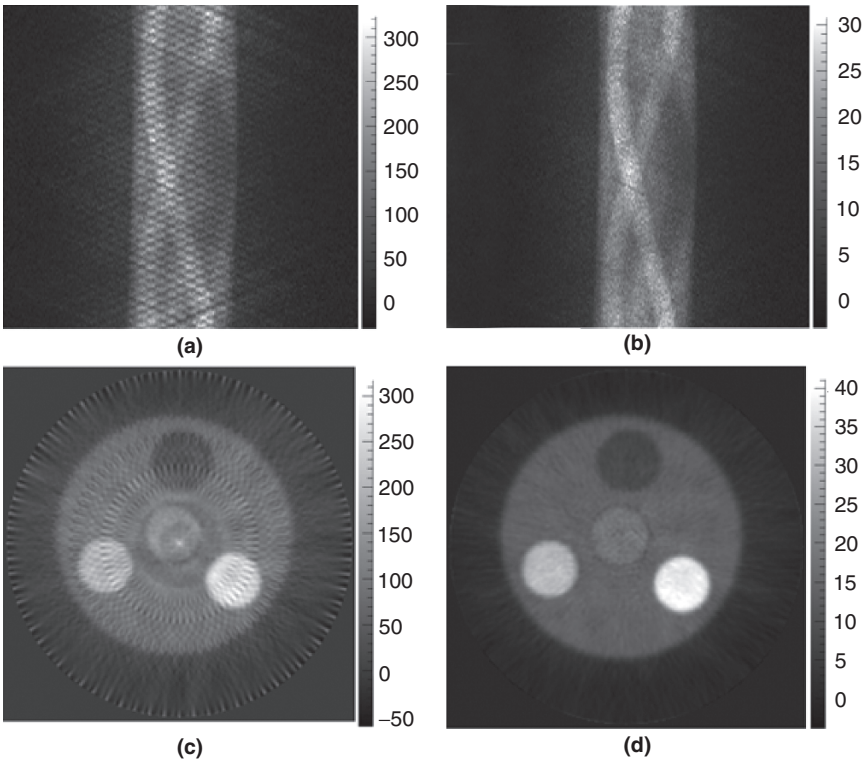

Fig. 2 Sinogram obtained from a NEMA whole body phantom scan. Upper left (**a**): no normalisation applied. Upper right (**b**): normalisation performed. Lower row: corresponding images reconstructed using a 3D filtered backprojection algorithm

2.2 Geometrical Corrections

Geometrical correction, also known as arc correction, is necessary to take into account the effectively different tangential bin sizes a given projection has. Different bin sizes result from the ring shaped arrangement of the detectors. The detectors at the edges of the projection appear smaller because their face side is inclined in respect to the projection axis. Variable tangential bin sizes are equivalent to different widths of the LoRs assembling the projection. This results in a non uniform sampling of the projection. The resolution at the edges of the field of view is deteriorated and artefacts occur. During arc correction the measured projections with non equal bin sizes are mapped onto projections with equal bin sizes by means of interpolation. Figure 3 shows the reconstructed image from a phantom consisting of 29 line sources homogenously distributed among the field of view. Close to the edges strong blurring and star like artefacts appear if no arc correction is applied.

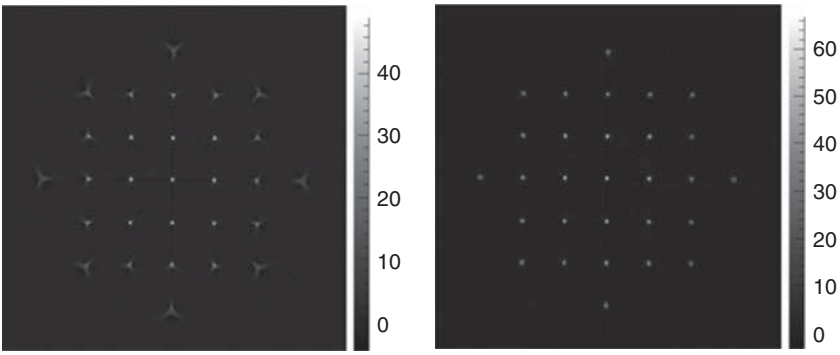

Fig. 3 Effects of arc correction. Left: no arc correction applied. Blurring and star like artefacts are clearly visible off z-axis. Right: same data and reconstruction with arc correction applied

2.3 Attenuation Correction

Photons travelling through matter can be absorbed. Absorption is a property of the media and the path length. In PET two photons are emitted back to back. Therefore, the total path length of the two photons is independent of the position on the LoR where the PET event occured. The probability that both photons reach the detectors is independent of their origin on the LoR. The attenuation correction factor for each projection bin or LoR can be estimated using transmission and blank scan. The correction factor for each detector pair is calculated by dividing blank through transmission scan. In practice the acquisition time of the transmission scan is in the order of a few minutes and therefore much shorter than the over night acquired blank scan. The different number of acquired events in each LoR needs to be considered. To avoid outlier the sinograms are smoothed, for example by median filtering. The EXACT HR+ scanner always acquires transmission and blank scan in 2D mode. For 3D data acquisition correction factors for oblique sinograms have to be derived from the 2D data sets. The used application does this by reconstructing attenuation images from the obtained attenuation correction sinograms using the 2D filtered backprojection algorithm. The resulting attenuation image is then forward projected into the oblique slices to get correction factors for the oblique sinograms. A calculated attenuation correction sinogram from a NEMA whole body phantom scan and the corresponding reconstructed attenuation image is shown in Fig. 4. In Fig. 5 images reconstructed from this data set with and without attenuation correction applied are displayed. It is clearly visible that the measured activity drops to around 50% of the expected activity towards the center of the phantom on the profiled line whereas a homogenous activity distribution is expected. The intensity drop in the reconstructed image disappears after applying attenuation correction to the emission sinograms.

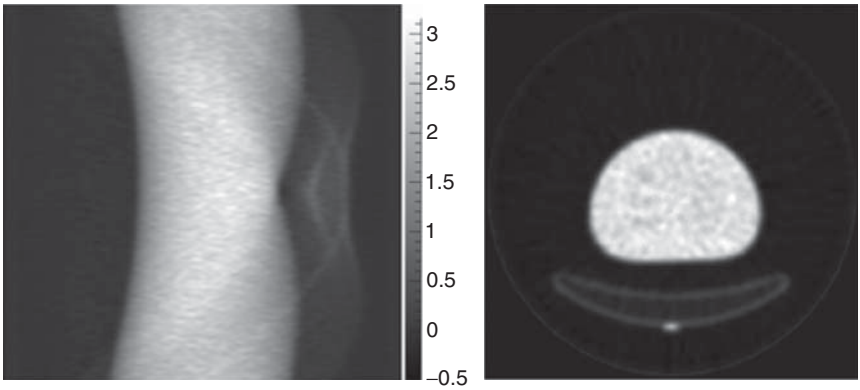

Fig. 4 Left: attenuation correction sinogram calculated from transmission and blank scan acquired during a scan of the NEMA whole body phantom. Right: reconstructed attenuation image

2.4 Scatter Correction

Photons travelling through tissue can not only be absorbed but also interact via scattering. A scattered photon will change its direction and thereby loose some of its energy depending on the scattering angle. Scattering will create false lines of response. A scattered photon can be discriminated because of its reduced energy. An energy window for photons is defined. Unfortunately, the energy resolution of the used scintillator materials is not good enough to suppress scatter completely. Scattered events cause background in the reconstructed image reducing the image contrast. Especially in quantitative PET scatter is a problem because the calculated absolute activities or standard uptake values (SUV) are falsified. In 3D PET up to 30% of the measured activity originates from scatter if no correction is applied[3]. A correction for scatter can be applied during the exercises by performing an object based scatter estimation using the SSS (single scatter simulation)-algorithm first introduced by Watson et al. in 1996.[4] The basic idea behind the algorithm is to get an estimate of the volume where scatter mainly occurs by reconstructing an attenuation image first. A certain number of elementary scatter volumes is distributed randomly inside the scatter volume.

The probability that a photon is scattered inside this volume, redirected and detected in another detector resulting in a false LOR is calculated using the Klein-Nishina formula. The amount of scatter in each LoR is estimated by summing up the contributions to each LoR from all elementary scatter volumes.[5] Figure 6 shows the image reconstructed from a Jaszczak phantom scan. No scatter correction is applied in the left image. An increasing background towards the center of the phantom is visible. After correcting the emission sinogram for scatter, the background is clearly reduced. The object or image based scatter correction can not eliminate scatter contributions originating from outside the FoV.

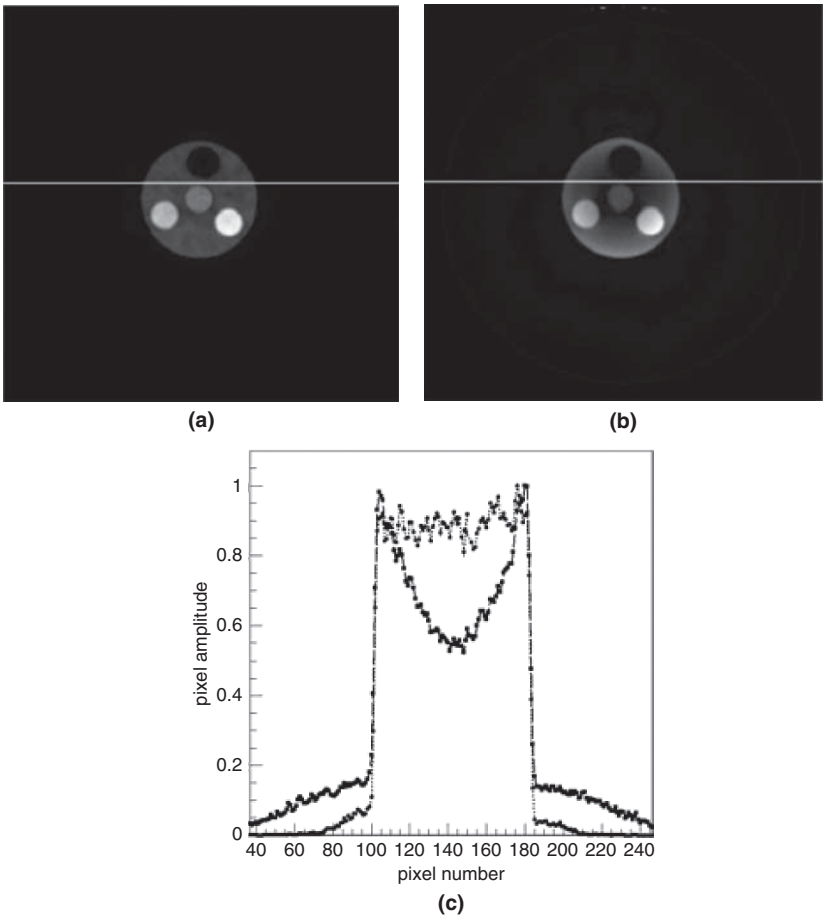

Fig. 5 Effect of attenuation correction. Along the profiled line the expected activity is constant. In case attenuation correction is performed the observed activity is nearly constant (**a**). If no attenuation correction is applied to the data the intensity drops visibly towards the center of the phantom (**b**). On the profiled line the activity drop is close to 50% (**c**)

3 Image Reconstruction

Two classes of reconstruction algorithms exist, analytical and iterative ones. The most popular analytical reconstruction method is the filtered backprojection (FBP) algorithm. The OSEM (ordered subset expectation maximisation) algorithm is the most popular iterative method used in clinical routine. Reconstruction algorithms were discussed in more detail in the lecture on PET image reconstruction preceding the exercises. All images shown in this chapter were acquired with a deluxe Jaszczak phantom with hot spot insert that was scanned with a Siemens/CTI EXACT HR+ scanner. The rods of the hot spot insert have diameters of 4.8, 6.4, 7.9, 9.5, 11.1,

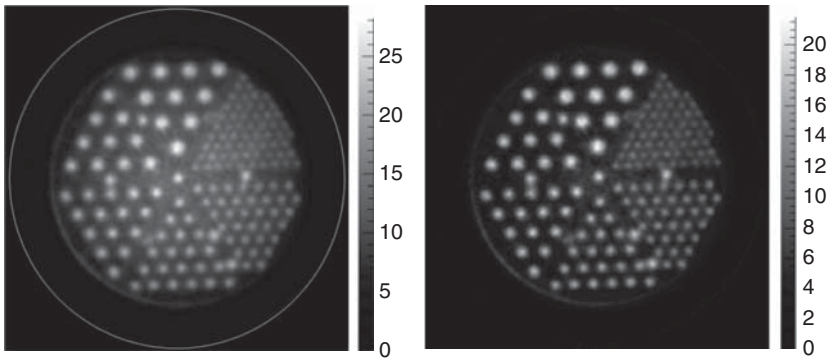

Fig. 6 Model based scatter correction using the SSS (single scatter simulation) algorithm. Left: no scatter correction applied. Right: scatter correction applied

12.7 mm. The phantom was filled with an aqueous solution of ^{18}F-FDG with an initial activity of 2.05 mCi. The data were acquired in standard 3D mode until 2.0 * 10^7 (low statistic acquisition) and 60 * 10^7(high statistic acquisition) counts were recorded.

3.1 Filtered Back Projection

Filtered back projection (FBP) is, as its name suggests, a combination of a filtering step performed on the projection data and a backprojection step. For 2D data all projections belonging to one z position are fourier transformed in respect to x_r using a FFT (fast fourier transform) algorithm. This data is then multiplied with a ramp filter and inverse fourier transformed back into projection space. The filtered projection is then backprojected onto the image. For more details see Defrise[6] and references therein. For 3D data sets the situation is more difficult due to the limited axial extend of the scanner. This causes incomplete data sets because of missing projections. This problem is overcome by the 3D reprojection algorithm (3DRP).[7] Missing projections are estimated from the activity distribution obtained by reconstructing the direct non oblique sinograms (a subset of the 3D data set). This estimation is then forward projected into those projections which do not exist in the real scanner. Therefore, this algorithm is also referred to as PROMIS (PROject MISsing data). The importance of the filtering step is demonstrated in Fig. 7.

Prerequisite for good image quality is a sufficient number of recorded PET events. Although this is a matter of course it is the first thing to look at if the image looks noisy and quality is in general bad with non of the artefacts visible described in the previous chapter. See Fig. 8.

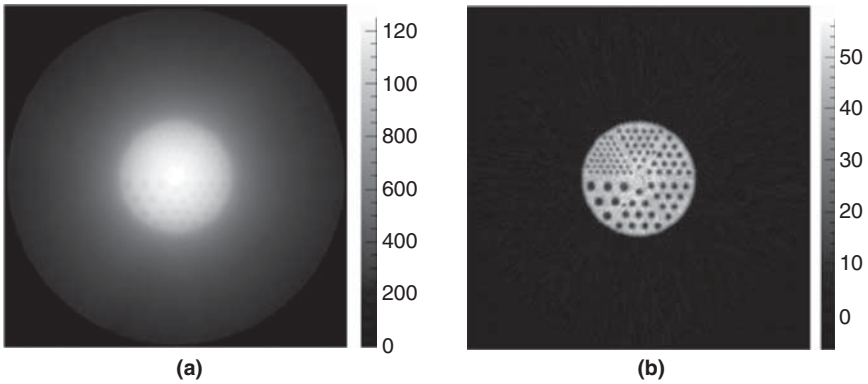

Fig. 7 Effects of the filtering step in 2D filtered back projection. (**a**) no ramp filter is applied to the projection data, simple backprojection. (**b**) ramp filtering of the projections before backprojection

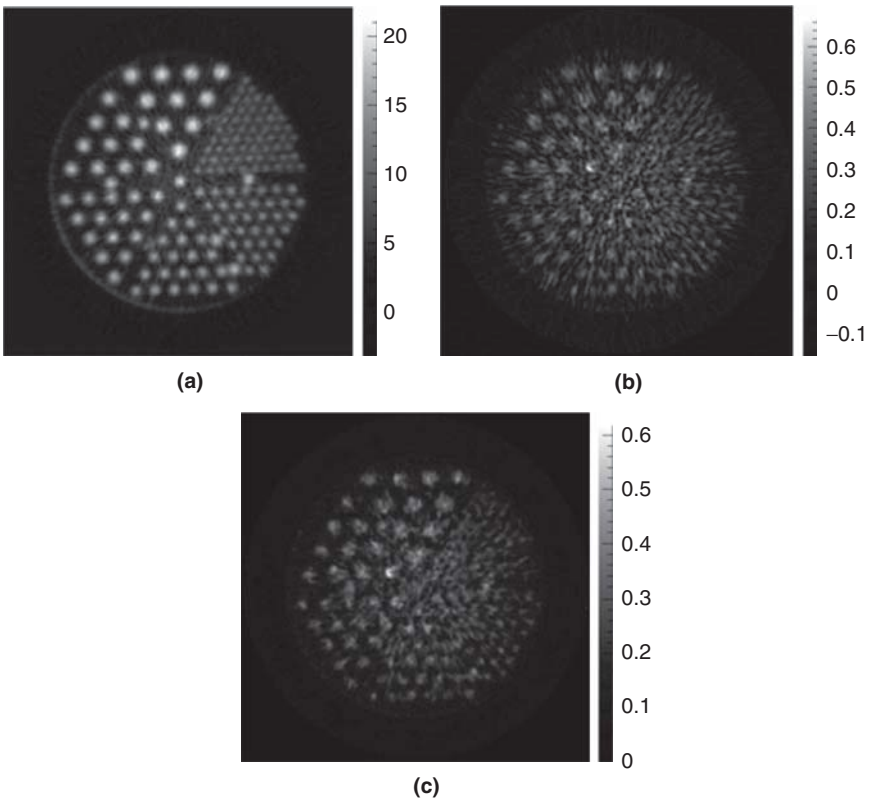

Fig. 8 (**a**) Image reconstructed from the high statistic scan using the 3DRP algorithm. Even the rods with the smallest diameter of 4.8 mm can be resolved. (**b**) the same for the scan with only a small number of events acquired using the FBP3D algorithm. Image (**c**) is reconstructed from the low statistic data set using the OSEM algorithm (12 subsets, 5 full iterations). Image quality is clearly dominated by scan statistics. In case of low statistics the iterative OSEM approach leads to better results due to the consideration of the statistical nature of the measured data in the reconstruction model compared to the analytical FBP3D algorithm

3.2 Iterative Approaches

In iterative image reconstruction the true activity distribution $f(x,y,z)$ is found by iteratively approximating the measured data with data derived from an estimated image. The initial estimation is usually a flat activity distribution normalised to one. The initial image is forward projected into the projections to get an estimation of what would have been measured by the scanner if this image had been the real one. Forward projection is the inverse operation of backprojection. It is done by summing up all amplitudes along a path forming a LoR. The LoRs are assembled to a sinogram which can be directly compared to the measured sinogram. Based on this comparison the estimated image is updated. Many approaches exist on how the comparison of the estimation and the measured data can be done and how to update the image estimate. The maximum likelyhood expectation maximization (MLEM) algorithm first proposed by Shepp and Vardi[8] is one of the most popular ones. It considers the statistical nature of PET data acquisition by means of Poisson statistics and by assigning different weights depending on the number of counts in a LoR. In MLEM each iteration requires forward projection and backprojection of the complete data set.

This is computationally expensive and convergence is slow. Ten to 100 iterations are required. Hudson and Larkin[9] developed an accelerated version of the EM algorithm based on the concept of ordered subsets (OSEM). The full data set containing all projections is split up in a certain number of subsets. These subsets are reconstructed successively and the image update step is done after each processed subset. The speed of convergence is greatly increased while the image quality remains similar to a MLEM reconstruction. The convergence behaviour as a function of the number of full iterations can be seen in Fig. 9. A typical choice for the number of subsets is between 2 and 20. Figure 10 shows the convergence of the OSEM algorithm with a fixed number of iterations as a function of the number of subsets chosen.

4 Conclusions

Several considerations are required to obtain high quality PET images. The PET scanner itself has to be set up properly and the individual detector responses have to be determined and quantified correctly. Before applying any reconstruction algorithm, the acquired data has to be normalised and arc corrected. If transmission scans were performed attenuation correction factors can be calculated. Especially in quantitative PET a correction for scatter is important. As far as possible this is done during the data acquisition itself by defining an energy window on the detected photons. In addition object based scatter corrections can be calculated offline. The image quality strongly depends on the number of acquired PET events. Low statistics always results in bad image quality. Statistics is the prevailing factor to image quality in clinical PET due to limited acquisition times and activities.

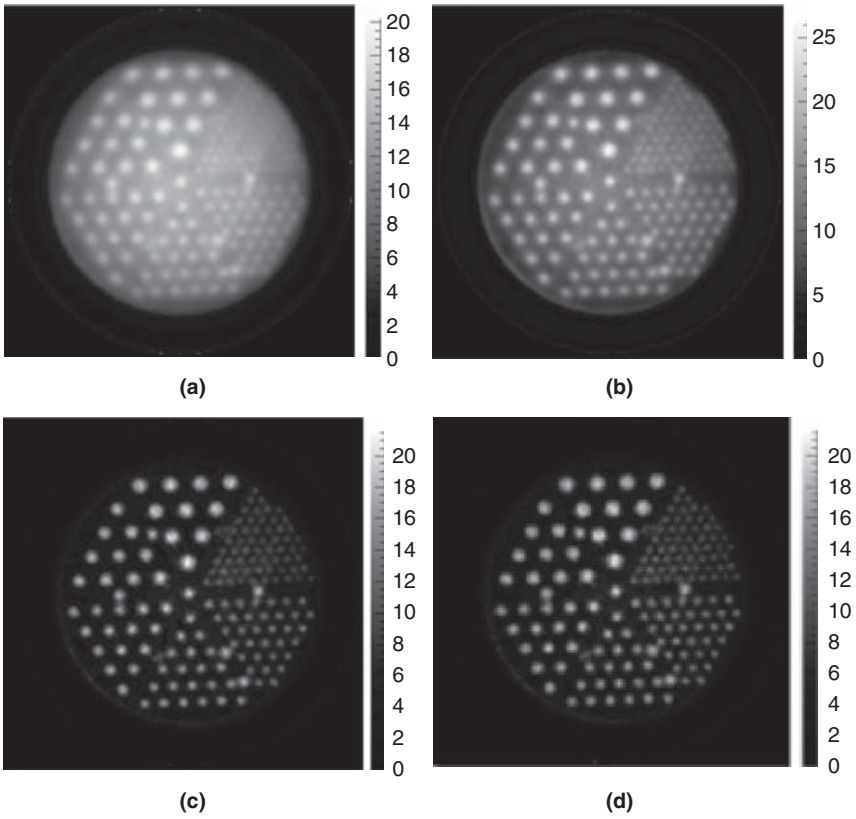

Fig. 9 Images reconstructed using the OSEM algorithm as a function of the number of full iterations performed. Number of subsets is 12. (**a**) 1 iteration, (**b**) 3 iterations, (**c**) 6 iterations and (**d**) 10 iterations

A clever choice of the reconstruction algorithm and its parameters is therefore essential. Iterative algorithms, like OSEM, are the preferred choice in case of limited statistics. The most important parameters in iterative reconstruction are the number of iterations and the choice of the number of subsets. If the number of iterations performed is too small, the image will look blurred and constrast is low. If too many iterations are performed, noise will be amplified. The optimum number of iterations in OSEM depends on the number of subsets chosen. The smaller the number of subsets, the more iterations are needed. The exercises were intended to mediate a first impression on all of the mentioned aspects. Without considering them properly, the resulting PET images will be suboptimal.

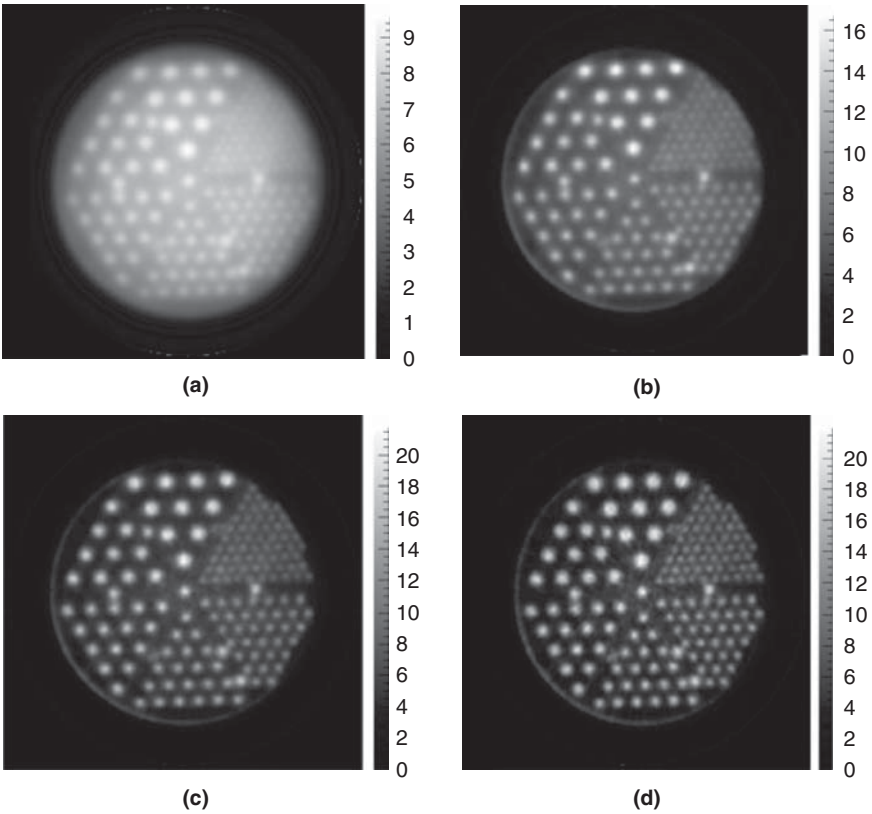

Fig. 10 Convergence of the OSEM algorithm as a function of the number of subsets used. The number of performed iterations is 5. (**a**) MLEM (1 subset), (**b**) 4 subsets, (**c**) 9 subsets and (**d**) 18 subsets. The larger the number of subsets the faster the convergence. The number subsets chosen and the number of full iterations performed must be balanced. If the number of subsets and iterations is too small the algorithm will not have converged resulting in a low contrast blurred image. See (a), (b). If the number of subsets is too large in respect to the number of full iterations (or vice versa) noise will be enhanced and the image will be increasingly grainy. See (d)

Acknowledgements The author likes to thank Dr. J. Doll for his help in acquiring the phantom data used during the exercises.

References

1. Labbé, C., Thielemans, K., Belluzzo, D. et al.: An Object-Oriented Library for 3D PET Reconstruction Using Parallel Computing. In: Evers, H., Glombitza, G., Lehmann, T., Meinzer, H.-P. (Eds.):*Informatik aktuell*, Springer (1999) pp. 268–272
2. Hammersmith Imanet, "STIR Software for Tomographic Image Reconstruction", Last update, 01/26/06. Available from: http://stir.sourceforge.net/

3. Adam, L.E., Zaers, J., Ostertag, H., et al.: Performance Evaluation of the whole-body pet scanner ECAT EXACT HR+ following the IEC standard. *IEEE Trans Nucl Sci* **44** (1997) 1172–1179
4. Watson, C.C., Newport, D., Casey, M.E., deKemp, R.A., Beanlands, R.S., Schmand, M.: Evaluation of simulation-based scatter correction for 3-D PET cardiac imaging.*IEEE Trans Nucl Sci* **44** (1997) 90–97
5. Werling, A., Bublitz, O., Doll, J., Adam, L.-E., Brix, G.: Fast implementation of the single scatter simulation algorithm and its use in iterative image reconstruction of PET data. *Phys Med Biol* **47** (2002) 2947–2960
6. Defrise, M., Kinahan, P.E.: Data Acquisition and Image Reconstruction for 3D PET. In: Bendriem, B., Townsend, D.W. (Eds.): *The Theory and Practice of 3D PET*. Kluwer, Dordrecht, The Netherlands/Boston, MA/London (1998)
7. Kinahan, P.E., Rogers, J.G.: Analytic 3D image reconstruction using all detected events. *IEEE Trans Nucl Sci* **36** (1989) 964–968
8. Shepp, L.A., Vardi, Y.: Maximum likelihood reconstruction for emission tomography.*IEEE Trans Med Imag* **MI-1** (1982) 113–122
9. Hudson, H.M., Larkin, R.S.: Accelerated image reconstruction using ordered subsets of projection data.*IEEE Trans Med Imag* **13** (1994) 601–609